

Paracrine Engineering of Human Cardiac Stem Cells With Insulin-Like Growth Factor 1 Enhances Myocardial Repair

Robyn Jackson, MSc; Everad L. Tilokee, MSc; Nicholas Latham, MSc; Seth Mount, BSc; Ghazaleh Rafatian, MSc; Jared Strydhorst, MSc; Bin Ye, MSc; Munir Boodhwani, MD; Vincent Chan, MD; Marc Ruel, MD; Terrence D. Ruddy, MD; Erik J. Suuronen, PhD; Duncan J. Stewart, MD; Darryl R. Davis, MD

Background—Insulin-like growth factor 1 (IGF-1) activates prosurvival pathways and improves postischemic cardiac function, but this key cytokine is not robustly expressed by cultured human cardiac stem cells. We explored the influence of an enhanced IGF-1 paracrine signature on explant-derived cardiac stem cell–mediated cardiac repair.

Methods and Results—Receptor profiling demonstrated that IGF-1 receptor expression was increased in the infarct border zones of experimentally infarcted mice by 1 week after myocardial infarction. Human explant-derived cells underwent somatic gene transfer to overexpress human IGF-1 or the green fluorescent protein reporter alone. After culture in hypoxic reduced-serum media, overexpression of IGF-1 enhanced proliferation and expression of prosurvival transcripts and prosurvival proteins and decreased expression of apoptotic markers in both explant-derived cells and cocultured neonatal rat ventricular cardiomyocytes. Transplant of explant-derived cells genetically engineered to overexpress IGF-1 into immunodeficient mice 1 week after infarction boosted IGF-1 content within infarcted tissue and long-term engraftment of transplanted cells while reducing apoptosis and long-term myocardial scarring.

Conclusions—Paracrine engineering of explant-derived cells to overexpress IGF-1 provided a targeted means of improving cardiac stem cell–mediated repair by enhancing the long-term survival of transplanted cells and surrounding myocardium. (*J Am Heart Assoc.* 2015;4:e002104 doi: 10.1161/JAHA.115.002104)

Key Words: cell survival • cell therapy • heart failure • insulin-like growth factor 1

Recent advances have fueled interest in the development of ex vivo proliferated resident cardiac stem cells (CSCs) as a cell candidate for myocardial repair.¹ This approach is teleologically pleasing because CSCs may provide a “natural” means of replacing damaged cardiomyocytes. Given the modest retention and long-term survival of transplanted CSCs,² several studies have suggested that the majority of benefits after CSC transplantation are driven largely by paracrine effects.^{3–5} It follows that strategies designed to broaden the paracrine signature of transplanted cells capable

of directing myogenesis may further enhance cell-mediated repair of injured myocardium; however, this remains to be shown because prevailing dogma stipulates that altering the paracrine profile of CSCs blunts regenerative performance.⁶

Insulin-like growth factor 1 (IGF-1) is a key cardioprotective cytokine that plays a vital role in early growth and development, with ongoing lifelong anabolic effects via the Protein kinase B and Extracellular Signal-Regulated Kinase/Mitogen-Activated Protein Kinase (ERK/MAPK) prosurvival pathways.^{7,8} Straightforward intracardiac injection of IGF-1 or blood-derived stem cells that overexpress IGF-1 into models of cardiac damage has been shown to decrease cell death and limit infarct expansion,^{9–11} suggesting that IGF-1 may provide a targeted means of promoting postinfarct cardiac repair.

We explored the influence of genetically enhancing the paracrine production of IGF-1 using human CSCs in an immunodeficient mouse model of myocardial ischemia. In this study, we used explant-derived cells (EDCs), which represent the earliest precursor cells that spontaneously emigrate from plated cardiac biopsies before prolonged ex vivo expansion¹² or antigenic selection.¹³ As detailed in previous publications, this cell product provides a cardirotrophic cell source that enhances postinfarct repair through direct differentiation to a

From the University of Ottawa Heart Institute, Ottawa, Canada (R.J., E.L.T., N.L., S.M., G.R., J.S., B.Y., M.B., V.C., M.R., T.D.R., E.J.S., D.R.D.); Ottawa Hospital Research Institute, Ottawa, Canada (D.J.S.).

An Accompanying Figures S1 through S5 and Tables S1 and S2 are available at <http://jaha.ahajournals.org/content/4/9/e002104/suppl/DC1>

Correspondence to: Darryl R. Davis, MD, University of Ottawa Heart Institute, H3214 40 Ruskin Ave, Ottawa, Ontario, Canada K1Y4W7. E-mail: ddavis@ottawaheart.ca

Received April 15, 2015; accepted August 12, 2015.

© 2015 The Authors. Published on behalf of the American Heart Association, Inc., by Wiley Blackwell. This is an open access article under the terms of the Creative Commons Attribution-NonCommercial License, which permits use, distribution and reproduction in any medium, provided the original work is properly cited and is not used for commercial purposes.

cardiac phenotype while providing indirect myocardial repair through paracrine-mediated repair (reviewed by Gago-Lopez et al¹⁴). Although previous attempts have been made to enhance myocardial IGF-1 content after myocardial infarction (MI) using transplanted cells, the use of an EDC approach avoids using cells that are notoriously difficult to genetically modify or that are unable to adopt a cardiac fate following transplantation.^{11,15} Furthermore, by using a cell source that can be naturally eliminated by the immune system in event of harm, we avoided unpredictable and potentially harmful effects to injured myocardium¹⁰ as well as the need for repeated administration.⁹ Unlike previous studies of genetically engineered CSCs,⁶ lentiviral-mediated somatic gene transfer would target the mesenchymal subpopulation within explant-derived CSCs (ie, the CD90+ subpopulation), which is thought to contribute little to the regenerative performance of explant-derived CSCs,^{14,16} and avoid detrimental effects on the cardiac and endothelial progenitor subpopulations within EDCs. We anticipated that targeted delivery of an IGF-1-enhanced paracrine signal by transplanted EDCs would boost the survival of transplanted cells to increase the generation of new cardiomyocytes from transplanted cells and increase the paracrine-mediated salvage of reversibly damaged tissue and recruitment of endogenous progenitor cells.

Methods

Effects of MI on IGF-1 Receptor Expression

After approval from the University of Ottawa Animal Care Service review board, 27 C57/BL6 mice (Charles River Laboratories International, Wilmington, MA, USA) were randomized to undergo thoracotomy with left anterior descending artery ligation (n=24) or control sham thoracotomy with no artery ligation (n=3). Mice were sacrificed 1, 7, 14, and 21 days after MI (n=3 per time interval), and the heart was microdissected into the infarct, infarct border zone, and off-target (posterior wall) regions. RNA was isolated using TRIzol for quantitative polymerase chain reaction (qPCR) of IGF-1 receptor (IGF-1R) and insulin receptor (IR) expression using commercial PrimeTime qPCR Assays and Primers (Integrated DNA Technologies). IGF-1R and IR transcript expression was normalized to GAPDH and presented as a fold change over sham-operated animals. Immunohistochemistry was used to confirm IGF-1R and IR expression, using commercial antibodies for IGF-1R (ab131476; Abcam), IR (ab137747; Abcam), and cardiac troponin T (ab10214; Abcam).

Cell Culture

Human EDCs were cultured from atrial appendage specimens obtained during clinically indicated procedures after informed

consent under a protocol approved by the University of Ottawa Heart Institute research ethics board. Atrial appendages were processed, as described previously.^{17–21} Briefly, tissue was cut into fragments, partially digested with collagenase IV (1 mg/mL; GIBCO), and plated within cardiac explant media (Iscove's modified Dulbecco's medium, 20% fetal bovine serum, 100 U/mL penicillin G, 100 µg/mL streptomycin, 2 mmol/l L-glutamine, and 0.1 mmol/L 2-mercaptoethanol; GIBCO). During the first week of culture, a layer of loosely adherent cells emerged from the plated cardiac tissue and were harvested using mild enzymatic digestion (0.05% trypsin; GIBCO). Each specimen underwent cell harvest up to 4 times. The collected heterogeneous EDC product was characterized for expression of cardiac progenitors (c-Kit; FAB332A; RD Systems), mesenchymal progenitors (CD90; 555596; BD Biosciences), IGF-1R (ab131476; Abcam), and IR (ab137747; Abcam) using flow cytometry (Guava easyCyte 8HT; EMD Millipore). A minimum of 40 000 events were collected with fluorescent compensation performed using single labeled controls (Flow-Jo v7.2.2; Treestar). The colorimetric WST-8 assay (Dojindo) was used to track cell viability and proliferation.

Cloning and Lentiviral Transduction

A third-generation lentiviral vector system was used to overexpress mature IGF-1 in concert with green fluorescent protein (GFP; lvIGF-1) or the GFP reporter only (lvGFP) as a null transduction control. Commercially sourced human IGF-1 cDNA (NM_001111283; GenScript Inc) was PCR amplified (TopTaq; Qiagen) and inserted into the backbone with transgene expression under control of the cytomegalovirus promoter (Verma Lab, Salk Institute for Biological Studies).²² Protein BLAST indicated >90% homology between human and murine IGF-1, obviating concerns regarding the use of xenogeneic insert. Lentivirus was generated using HEK293 cotransfection followed by viral suspension filter-column concentration (Centricon Plus-70; Millipore). Viral titers were verified using qPCR for lentiviral particles.²³

As demonstrated in Figure 1, the CD90+ subpopulation within EDCs was immunomagnetically sorted (Life Technologies) using a human-specific CD90+ antibody (555596; BD Biosciences) and cultured in parallel from the CD90–depleted fraction. CD90+ cells were transduced with lvIGF-1 or lvGFP, and both subpopulations were recombined after 48 hours.

The influence of somatic gene transfer on the paracrine signature of EDCs was evaluated in conditioned media using enzyme-linked immunosorbent assay (DG100; R&D Systems) or protein array profiling (G-Series Human Cytokine Antibody Array kit; RayBiotech). Conditioned media was obtained after 48 hours of culture in hypoxic (1% oxygen), low-serum (1%

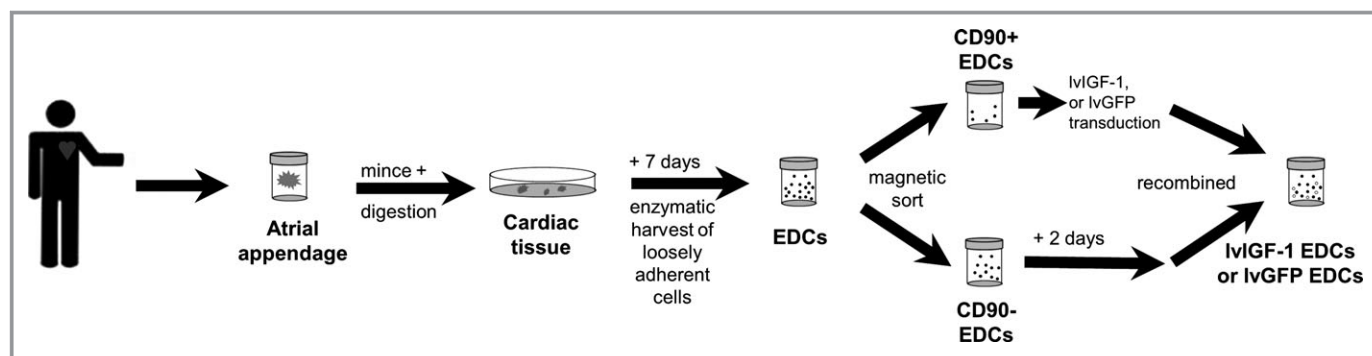


Figure 1. Study design. Schema of the study design highlighting cell source, CD90-guided magnetic separation, and transduction (lvGFP or lvIGF-1) prior to recombination for further experimentation. EDC indicates explant-derived cell; lvGFP, lentiviral-mediated overexpression of the green fluorescent protein reporter; lvIGF-1, lentiviral-mediated overexpression of mature IGF-1 with green fluorescent protein.

serum) conditions to simulate the environment of the infarcted myocardium. All immunosorbent measures were normalized to media volume and protein cell lysate.

Effects of IGF-1 on Cell Death

The capacity to IGF-1–engineered EDCs to withstand cell death was assessed after culture in hypoxic (1% oxygen), low-serum (1% serum) conditions for 48 hours by examining (1) proliferation using the WST-8 assay (Dojindo); (2) expression of early apoptotic markers using flow cytometry (559763; BD Biosciences); (3) expression of Bcl-2, Fos, and Jun pro-survival transcripts using qPCR (Integrated DNA Technologies); (4) expression of 35 apoptosis-related and stress-activated proteins using a membrane-based antibody array (ARY009; R&D Systems); and (5) expression of necroptosis markers (RIP1, ab106393; RIP3, ab152130; caspase-8, ab25901; FADD, ab24533; Abcam) using Western blot densitometry.

The pro-survival effect of IGF-1 overexpression on neighboring myocardium was explored during direct and indirect (Transwell; Corning) coculture with neonatal rat ventricular myocytes (NRVMs; R-CM-561; Lonza). EDCs were distinguished from NRVMs using Vybrant DiO Cell-Labeling Solution (Molecular Probes). NRVMs and EDC cocultures underwent analysis of (1) cell viability using the colorimetric WST-8 assay, (2) apoptosis using flow cytometry for annexin V, and (3) expression of the antiapoptotic protein Bcl-2 (ab692; Abcam) using immunohistochemistry.

MI, Cell Injection, and Effects of Cell Therapy

At 1 week after left anterior descending artery ligation, NOD SCID mice (6 weeks old; Charles River Laboratories International) were randomized to receive intramyocardial injection of lvGFP-transduced EDCs ($n=9$), lvIGF-1–transduced EDCs ($n=8$), or inactive vehicle (PBS; $n=9$).^{18,19,24} Echocardiographic guidance (VisualSonics V1.3.8 software) was used for

intramyocardial injection of 100 000 EDCs or PBS, divided between the apex and lateral infarct border zone. All mice underwent echocardiographic imaging at 14 and 21 days after cell transplantation, with left ventricular chamber dimensions and ejection fraction calculated from the parasternal images using standard techniques.^{18,19,24} Quantitative morphometry and scar burden was assessed 21 days after cell injection using Masson's trichrome staining (Life Technologies).

The spatiotemporal progression of human IGF-1 expression was characterized in a separate series of NOD SCID mice after transplantation of lvGFP- or lvIGF-1–transduced EDCs. These mice were sacrificed 1, 7, and 14 days after cell injection ($n=3$ per group). Peripheral blood was obtained prior to euthanasia to evaluate circulating levels of human IGF-1. The ventricles were microdissected into the infarct, infarct border zone, and off-target (posterior wall) regions for simultaneous DNA, protein, and mRNA extraction using TRIzol (Life Technologies). IGF-1 transcript expression was assessed using commercial primers (Integrated DNA Technologies), whereas EDC engraftment was verified using qPCR for noncoding human Alu sequences.^{18,19,25} To evaluate the influence of enhanced IGF-1 expression on apoptosis, qPCR expression of Bcl-2, Bax, and p53 transcripts 7 days after EDC injection was evaluated using commercial primers (Integrated DNA Technologies).

The effects of EDCs on myocardial perfusion and apoptosis were characterized in separate series of NOD SCID mice after injection of EDCs (lvGFP or lvIGF-1) or vehicle (PBS) 1 week after left anterior descending artery ligation ($n=3$ mice per group). Single-photon emission computed tomography (SPECT)/computed tomography imaging was performed 1 day prior to EDC injection and 2 days after EDC injection. Prior to imaging (NanoSPECT/CT; Mediso), all mice were injected with 1.91 ± 0.55 mCi of ^{99m}Tc -rhAnnexin V-128 (Atreus Pharmaceuticals). Next, 48 equally spaced projections following a helical trajectory were acquired for 150 seconds per projection (2 scans summed for total scan time ≈ 1 hour).

Following acquisition of the ^{99m}Tc -rhAnnexin V-128 projections, mice were injected with 0.42 ± 0.07 mCi of ^{201}Tl and imaged for 20 minutes. MicroSPECT images were reconstructed with HiSPECT provided by the camera manufacturer and analyzed with 4DM-SPECT (Invia). Wall contours were detected based on ^{201}Tl uptake and copied to the ^{99m}Tc -rhAnnexin V-128 images. Based on these contours, grayscale 17-segment polar maps for both tracers were created. Infarct size and ^{99m}Tc -rhAnnexin V-128 uptake were calculated (MATLAB; MathWorks). Infarct size was calculated as the fraction of pixels of the left ventricle with an intensity $<50\%$ of the maximum intensity. The mean uptake ratio for ^{99m}Tc -rhAnnexin V-128 is the ratio of the average Tc-annexin uptake in those pixels in which the ^{201}Tl uptake was $<50\%$ of maximum to the background uptake. Background uptake of ^{99m}Tc -rhAnnexin V-128 was defined as the mean uptake in the septal segments of the basal slice. On completion of SPECT imaging, all animals were sacrificed for qPCR analysis of Bax and p53 expression within the infarct and peri-infarct regions.

To monitor endogenous repair, a series of NOD SCID mice ($n=15$) were injected with bromodeoxyuridine (BrdU; 100 mg/kg IP) once daily for 7 days after intramyocardial injection of EDCs or vehicle 1 week after MI. At 21 days after EDC or vehicle injection, mice were sacrificed and hearts were sent for immunohistochemical analysis of BrdU (ab6326; Abcam) cosegregation with cardiac troponin T (ab125266; Abcam).

Statistical Analysis

All data are presented as mean \pm SEM. To determine whether differences existed within groups, data were analyzed by 1-way or repeated-measures ANOVA; if such differences existed, Bonferroni's corrected t test was used to determine the groups with the differences (SPSS v20.0.0; IBM Corp). To account for multiple comparisons made from the serial echocardiograms, these functional data were analyzed using a repeated-measures mixed model with post hoc testing done using t tests, as appropriate, with Bonferroni's correction. In all cases, variances were assumed to be equal, and normality was confirmed prior to further post hoc testing. Differences in categorical measures were analyzed using Fisher's exact test. A final value of $P\leq 0.05$ was considered significant for all analyses.

Results

IGF-1R Expression Was Increased After MI

To identify the best time to administer IGF-1, the spatiotemporal expression of IGF-1R and IR was evaluated after experimental infarction. At 1, 7, 14, and 21 days after

proximal ligation of the left anterior descending artery, infarcted left ventricles were microdissected into the infarct, border zone, and off-target regions (posterior wall). As early as 24 hours after infarction, the expression of IGF-1R was increased 1.4 ± 0.7 -fold within the infarct border zone ($P=0.02$ versus sham-operated mice) (Figure 2A). IGF-1R expression remained elevated through the 21-day sampling period, with peak expression detected 7 to 14 days after artery ligation within the infarct zone (3.0 ± 0.8 and 4.1 ± 1.7 -fold increase, respectively; $P\leq 0.05$ versus sham-operated mice). Immunohistochemical imaging of postinfarcted sections confirmed similar widespread expression of IGF-1R within the ischemic border zone and infarct region (Figure 2B and Figure S1). In contrast, IR was rarely observed and did not significantly change in response to myocardial injury (Figure 2A). Taken together, these data suggest that IGF-1R expression is enhanced for at least 21 days after infarction and rationalize the timing of IGF-1 delivery to the infarcted myocardium.

Baseline Demographics

Ten patients donated myocardial biopsies for this study (age 66 ± 3 years; body mass index 29 ± 2 kg/m 2) (Table S1). Although all 10 patient cell lines were used for in vitro experimentation, only 6 randomly selected cell lines were

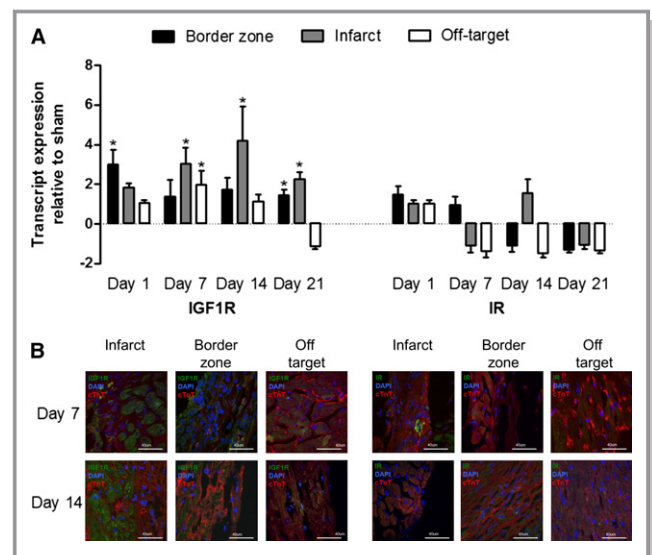


Figure 2. Spatiotemporal expression of IGF-1R and IR after left anterior descending artery ligation. A, Quantitative reverse transcription polymerase chain reaction of IGF-1R and IR expression at 1, 7, 14, and 21 days after MI with mRNA transcript expression normalized to mice undergoing a sham operation. $*P\leq 0.05$ vs sham-operated mice; $n=3$ mice per sampling interval. B, Representative immunohistochemical images of infarct, border zone, and off-target myocardium at 7 and 21 days after MI. IGF-1R indicates insulin-like growth factor 1 receptor; IR, insulin receptor; MI, myocardial infarction.

used in the *in vivo* experiments (*P* value not significant for differences in clinical variables between groups). Although long-term glucose control differed between diabetic and nondiabetic patients, all EDC lines served as their own controls to minimize the influence of hyperglycemic control on study outcomes.²⁴ Flow cytometry of representative fractions from each cell line demonstrated proportions of cardiac and mesenchymal progenitors consistent with previous publications (Figure S2A).^{17–21,24}

CSCs Produced Modest Amounts of IGF-1 and Expressed IGF-1Rs

Although human EDCs naturally produce low levels of IGF-1 (149±16 pg/mL, 3 EDC lines), the source of this cytokine is unknown. Subculture of isolated cardiac progenitor cells (c-Kit+/CD90–), mesenchymal progenitor cells (c-Kit–/CD90+), and lineage-negative cells (c-Kit–/CD90–) demonstrated that IGF-1 production was equivalent in all 3 cell populations (ANOVA, *P*=0.9). Interestingly, flow cytometry demonstrated that IGF-1R and IR were expressed by 79±3% and 61±5% of EDCs, respectively (Figure S2B). Of these, the cardiac (c-Kit+/CD90–) and mesenchymal (c-Kit–/CD90+) subpopulations had the greatest expression (chi-square test 17.2 and 12.1, respectively; *P*≤0.01 versus the expected frequency of IGF-1R or IR in the c-Kit–/CD90– subpopulation) (Figure S2C). These data demonstrate that EDCs produce modest amounts of IGF-1 and may be responsive to IGF-1 autocrine stimulation.

Somatic Gene Transfer Increased IGF-1 Secretion Without Blunting the Paracrine Signature of CSCs

EDCs were genetically engineered to overexpress IGF-1 by transducing isolated CD90+ cells prior to recombination with the CD90– depleted fraction (Figure 1). The mesenchymal CD90+ subpopulation within EDCs was selected as the platform for IGF-1 overexpression because it provides a reliable population of easily transduced cells that likely contributes very little to EDC-mediated myocardial repair.^{16,26} Interestingly, a recent publication¹⁴ provided additional context for this finding: CD90+ clones derived from cardiosphere-derived cells (an expanded progeny of EDCs) were shown to express markers consistent with a mesenchymal/myofibroblast cell, a phenotype that promotes maladaptive remodeling after MI.^{27–29} Finally, the decision not to simply transduce all complementary subpopulations within EDCs was based on emerging evidence suggesting that direct transduction of the entire EDC admixture disrupts the cytokine production of EDCs to ultimately impair cardiac repair.⁶ To control for effects attributable to lentiviral transduction, the CD90+

subpopulation from each cell line was transduced with the lvGFP vector prior to recombination. As demonstrated in Figure 3A, somatic gene transfer provided discreet GFP and IGF-1 transcripts without evidence of a fused GFP–IGF-1 product. Flow cytometry demonstrated that 83±2% of the transduced CD90+ cells expressed the lvIGF-1 GFP reporter 48 hours after transduction. The IGF-1 transcript content within recombined EDCs was increased by 3848±256-fold 48 hours after lvIGF-1 transduction (*P*=0.001 versus lvGFP-treated control cells). Conditioned media from recombined lvIGF-1–transduced EDCs demonstrated a multiplicity of infection–dependent increase in IGF-1 content that was sustained for 3 weeks in culture (Figure 3B). Lentiviral transduction with lvGFP or lvIGF-1 at a multiplicity of infection of 20 did not impair proliferation compared with nontransduced EDCs (population doubling time: 1.1±0.3 or 1.2±0.1 versus 2.5±1.5 days, respectively; *P* value not significant).

In contrast to lentiviral-mediated overexpression of hypoxia-inducible factor 1α,⁶ transduction of EDCs with lvIGF-1 did not significantly alter cytokine production (chi-square test 2.00, *P*=0.55 versus the expected frequency of cytokines in lvGFP-transduced EDCs) (Figure 3C). These data confirm the notion that transduction of the mesenchymal subpopulation within EDCs with lvIGF-1 provides a reliable reservoir to enhance IGF-1 content without impairing the overall cytokine profile of EDCs.

Overexpression of IGF-1 by CSCs Promoted CSC and Cardiomyocyte Survival

To evaluate the protective effect of IGF-1 on EDC survival in stress conditions, EDCs were exposed to hypoxic (1% O₂), reduced-serum (1%) conditions. EDCs genetically engineered to overexpress IGF-1 demonstrated enhanced proliferation compared with lvGFP-transduced and nontransduced EDCs (Figure 4A).

Given that IGF-1 has been shown to protect dystrophic myofibers from necrosis,³⁰ the expression of apoptotic and necroptotic markers were profiled in hypoxic EDCs. As shown in Figure 4B and Figure S3A, the necroptotic proteins RIP1 and RIP3 were not influenced by lvIGF-1, whereas drivers of apoptosis (caspase-8 and FADD) were significantly downregulated by 2.9±1.3 and 2.8±0.8-fold within lvIGF-1–transduced and nontransduced EDC cultures, respectively (*P*≤0.05). In support of these results, lvIGF-1–transduced EDCs cultured in hypoxic low-serum conditions enhanced stimulation within the AKT, ERK, and MAPK prosurvival pathways (*P*≤0.05 versus lvGFP-transduced or nontransduced EDCs) (Figure 4C). Furthermore, a commercial protein array of 35 apoptosis-related proteins demonstrated that downstream activators of these pathways (eg, Bcl-2, Bcl-x, survivin, and HSP70) were markedly

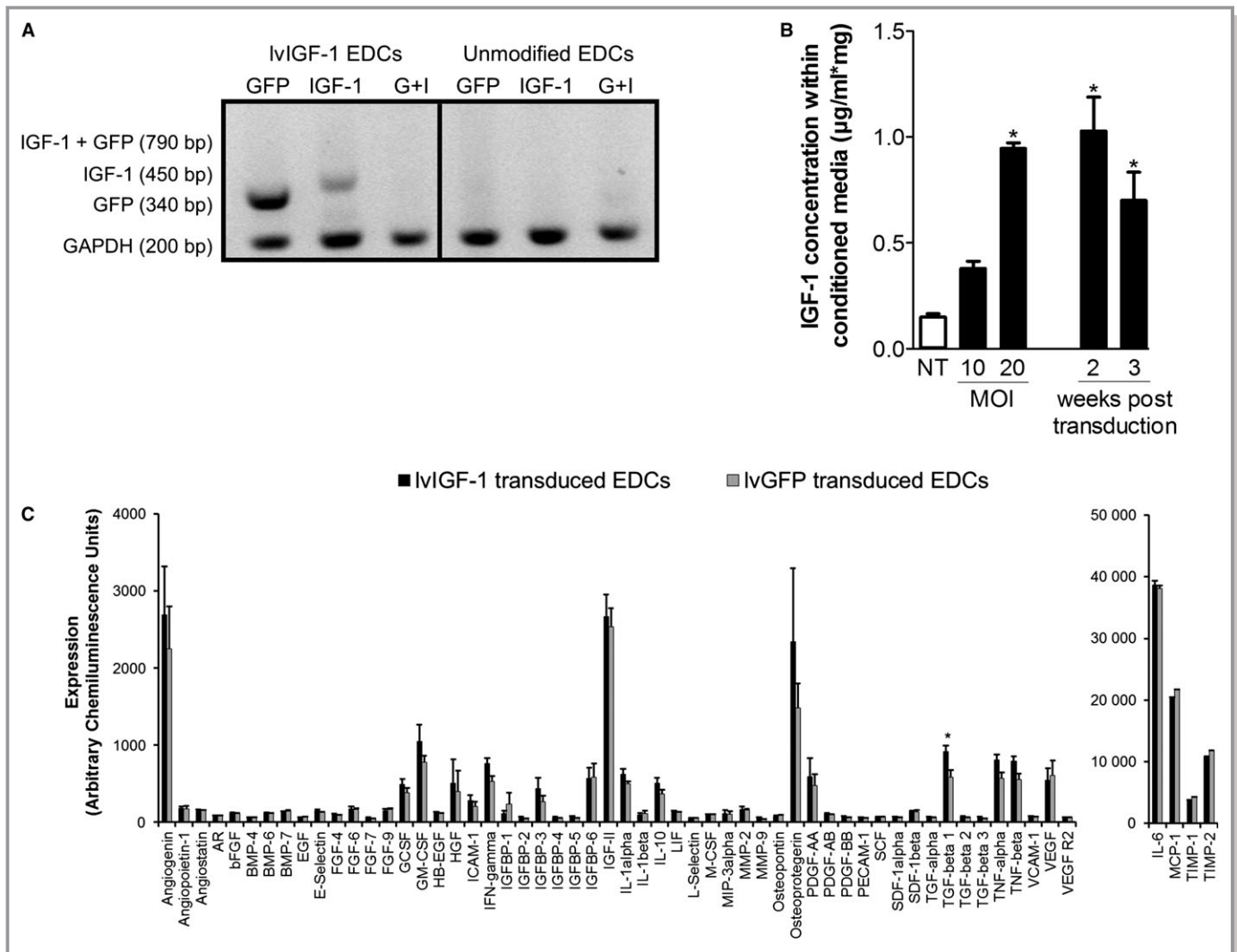


Figure 3. Lentiviral-mediated overexpression of human IGF-1 in EDCs. A, Quantitative polymerase chain reaction of lvIGF-1 and nontransduced unmodified EDCs demonstrating that somatic gene transfer provided discreet transcripts for GFP and IGF-1 without production of a GFP–IGF-1 fusion product. B, MOI-dependent human IGF-1 protein content within media conditioned by EDCs 48 hours after recombination of the lvIGF-1–transduced CD90+ subpopulation with the nontransduced CD90– subfraction. * $P \leq 0.05$ vs nontransduced EDCs; 4 EDC lines. C, Densitometry analysis of growth factors produced by lvIGF-1–transduced EDCs compared with lvGFP-transduced EDCs using a custom protein array. * $P \leq 0.05$ vs lvGFP-transduced EDCs; =4 EDC cell lines per lentiviral vector. AR indicates androgen receptor; bFGF, basic fibroblast growth factor; BMP, bone morphogenetic protein; bp, base pair; EDCs, explant derived cells; EGF, epidermal growth factor; FGF, fibroblast growth factor; G+I, GFP–IGF-1 fusion product; GCSF, granulocyte colony-stimulating factor; GFP, green fluorescent protein; GM-CSF, granulocyte macrophage colony-stimulating factor; HB-EGF, heparin binding epidermal growth factor; HGF, hepatocyte growth factor; ICAM-1, intracellular adhesion molecule; IFN, interferon; IGF-1, insulin-like growth factor 1; IGFBP-1, insulin-like growth factor-binding protein; IL, interleukin; LIF, leukemia inhibitory factor; lvGFP, lentiviral-mediated overexpression of the green fluorescent protein reporter; lvIGF-1, lentiviral-mediated overexpression of mature IGF-1 with green fluorescent protein; M-CSF, macrophage colony-stimulating factor; MCP-1, monocyte chemoattractant protein-1; MIP, macrophage inflammatory protein; MMP, matrix metalloproteinase; MOI, multiplicity of infection; NT, nontransduced; PDGF, platelet-derived growth factor; SCF, stem cell factor; SDF, stromal cell-derived factor; TIMP, tissue inhibitor of metalloproteinase; TGF, transforming growth factor; TNF, tumor necrosis factor; VCAM, vascular cell adhesion molecule; VEGF, vascular endothelial growth factor.

elevated in lvIGF-1–transduced EDCs (Figures 4C and 3B) ($P \leq 0.05$ versus lvGFP-transduced EDCs).

The effect of IGF-1 overexpression on myocyte preservation was modeled using NRVMs cultured under hypoxic low-serum (1% FBS) conditions. As shown in Figure 5A, lvIGF-1 EDC–conditioned media reduced NRVM cell loss compared

with NRVMs cultured in lvGFP or nontransduced EDC–conditioned media (-15.2 ± 4.7 versus -20.4 ± 2.9 and -24.1 ± 2.2 , respectively; $P \leq 0.01$) (Figure 5A). Direct and indirect (Transwell; Corning) culture of NRVMs with fluorescence-labeled EDCs confirmed that lvIGF-1–transduced EDCs reduced the expression of annexin V within both myocytes

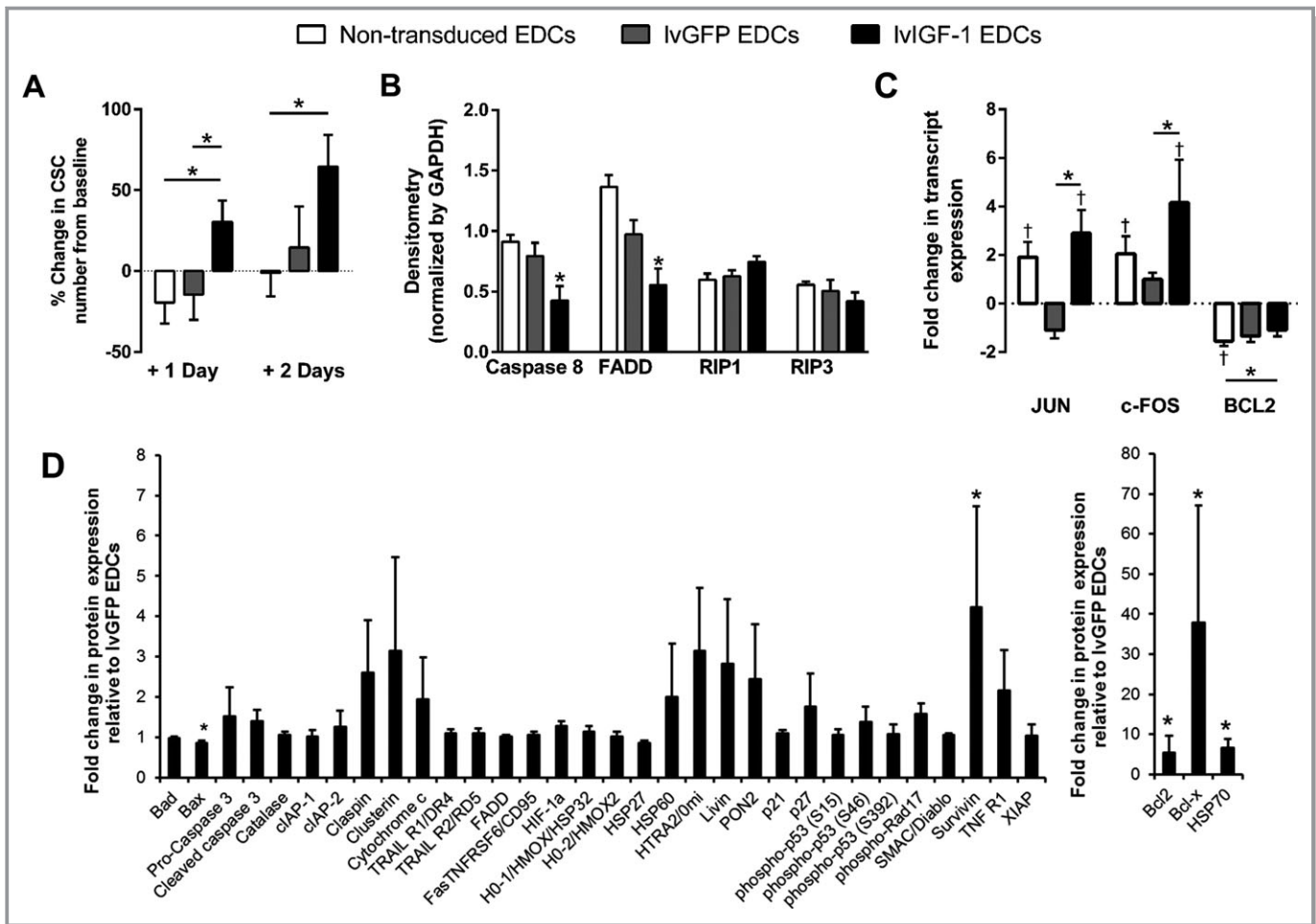


Figure 4. Overexpression of IGF-1 protects EDCs against apoptosis but not necroptosis. A, Change in the number of lvGFP-, lvIGF-1-, and nontransduced EDCs from the initial baseline count (>8 hours after plating) after exposure to hypoxic (1% oxygen), low-serum (1% FBS) conditions. * $P < 0.05$ vs lvGFP- or nontransduced EDCs; 9 EDC lines with 3 technical repeats. B, Densitometry analysis of Western blots demonstrating the effects of lvIGF-1 to protect against markers of apoptosis. * $P < 0.05$ vs nontransduced EDCs; 3 EDC lines with 2 technical repeats. C, Quantitative polymerase chain reaction analysis of MAPK/ERK and Akt signaling pathway activation within lvGFP-, lvIGF-1-, and nontransduced EDCs after 48 hours of exposure to hypoxic (1%) and low-serum (1% FBS) culture conditions. * $P < 0.05$ vs lvGFP- or nontransduced EDCs, † $P < 0.05$ vs normoxic EDCs (6 EDC lines with 3 technical repeats). D, Relative expression of 35 apoptosis-related and stress-activated proteins in lvIGF-1-transduced EDCs using a commercial human apoptosis proteome profiler array. Expression normalized to lvGFP-transduced EDCs. * $P < 0.05$ vs lvGFP-transduced EDCs; 4 EDC lines with 2 technical repeats. Bad indicates Bcl-2-associated death promoter; Bax, *BCL2-associated X*; Bcl-2, B-cell lymphoma 2; Bcl-x, B-cell lymphoma extra large; CIAP1, cellular inhibitor of apoptosis protein 1; CIAP2, cellular inhibitor of apoptosis protein 2; CSCs, cardiac stem cells; EDCs, explant-derived cells; FADD, Fas-Associated protein with Death Domain; Fas/TNFSF6, Fas Ligand/ tumor necrosis factor receptor 6; FOS, v-fos FBJ murine osteosarcoma viral oncogene homolog; HIF-1 α , Hypoxia-inducible factor 1-alpha; HO-1/HMOX1/HSP32, Heme Oxygenase 1/heme oxygenase (decycling) 1/ Heat Shock Protein 32; HO-2/HMOX2, Heme Oxygenase 2/heme oxygenase (decycling) 2; HSP27, Heat Shock Protein 27; HSP60, Heat Shock Protein 60; HSP70, Heat Shock Protein 70; HTRA2/Omi, High temperature requirement protein α 2/Omi stress regulated endoprotease; IGF-1, insulin-like growth factor 1; lvGFP, lentiviral-mediated overexpression of the green fluorescent protein reporter; lvIGF-1, lentiviral-mediated overexpression of mature IGF-1 with green fluorescent protein; p21/CIP1/CDKN1A, cyclin-dependent kinase inhibitor 1A; p27/Kip1, Cyclin-dependent kinase inhibitor 1B; Phospho-p53, phosphorylated tumor protein 53; PON2, paraoxonase 2; RIP1, Receptor-interacting protein 1; RIP3, Receptor-interacting protein 3; SMAC, Second Mitochondria-derived Activator of Caspases; TNF RI/TNFRSF1A, Tumor necrosis factor receptor 1/Tumor necrosis factor receptor superfamily member 1A; TNF, tumor necrosis factor; TRAIL R1/DR4, Tumor Necrosis Factor-Related Apoptosis-Inducing Ligand receptor 1/death receptor 4; TRAIL R2/DR5, Tumor Necrosis Factor-Related Apoptosis-Inducing Ligand receptor 2/death receptor 5; XIAP, X-linked inhibitor of apoptosis.

and cocultured EDCs ($P < 0.05$) (Figure 5B). This paracrine effect is further supported by the observation that exposure of NRVMs to lvIGF-1 EDC-conditioned media increased the

number of Bcl2+ NRVMs compared with culture within lvGFP or nontransduced EDC-conditioned media ($44.6 \pm 3\%$ versus $30 \pm 3\%$ and $25 \pm 3\%$, respectively; $P < 0.05$) (Figure 5C).

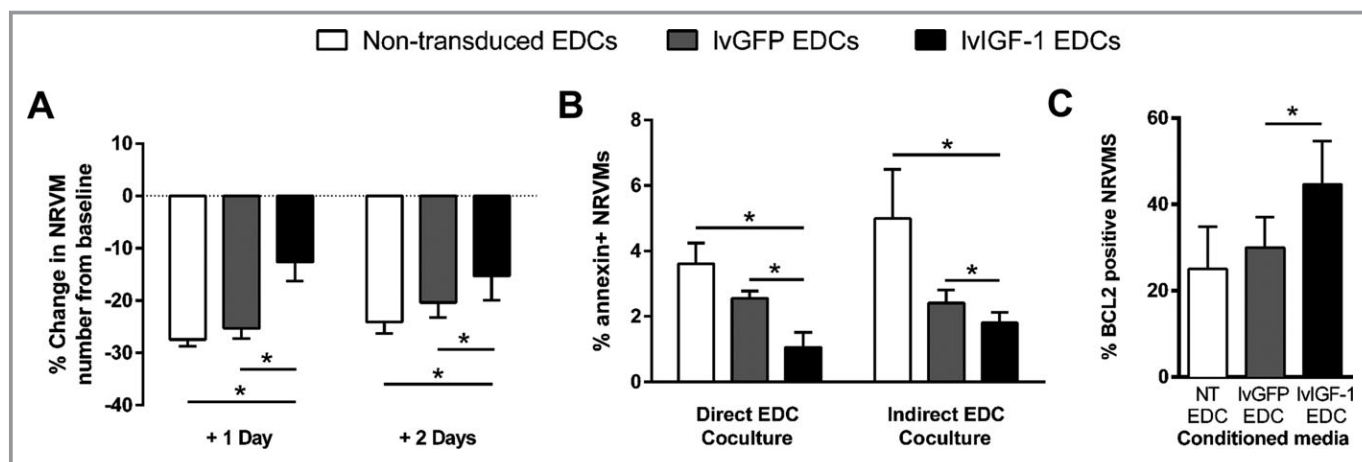


Figure 5. Overexpression of IGF-1 within EDCs enhances myocyte survival. A, Change in the number of NRVMs from the initial baseline count (>8 hours after plating) after culture in hypoxic (1% oxygen), low-serum (1% FBS) lvGFP-, lvIGF-1-, and nontransduced EDC-conditioned media. * $P \leq 0.05$ vs lvGFP- or nontransduced EDCs; 9 NRVM cultures with 3 technical repeats. B, Analysis of flow cytometry demonstrating the effect of IGF-1 overexpression on early markers of apoptosis (annexin V) of NRVMs when directly cocultured or indirectly cocultured with EDCs. Data are mean \pm SEM; 3 NRVM cultures with 2 technical repeats. * $P \leq 0.05$ vs lvGFP- or nontransduced EDCs. C, Random field analysis of BCL2 coexpression within NRVMs cultured with conditioned media from lvGFP-, lvIGF-1-, or nontransduced EDCs. * $P \leq 0.05$ vs lvGFP- or nontransduced EDCs; 3 NRVM cultures with 3 random fields per culture. EDC indicates explant derived cell; IGF-1, insulin-like growth factor 1; lvGFP, lentiviral-mediated overexpression of the green fluorescent protein reporter; lvIGF-1, lentiviral-mediated overexpression of mature IGF-1 with green fluorescent protein; NRVMs, neonatal rat ventricular myocytes; NT, nontransduced.

Taken together, these data suggest that overexpression of IGF-1 within human EDCs may play a role in protecting EDCs from apoptotic cell death, with little influence on necroptotic cell death. Furthermore, these data suggest that transplantation of lvIGF-1-transduced EDCs may provide autocrine support to promote the survival of transplanted EDCs while protecting the surrounding myocardium against apoptotic cell loss during postinfarct healing.

Overexpression of IGF-1 by CSCs Enhanced Cardiac Repair and Engraftment of Transplanted CSCs

The effect of lvIGF-1-transduced EDCs on cardiac repair was assessed in an immunodeficient mouse model of myocardial ischemia. As shown in Figure 6A, transplantation with either lvIGF-1- or lvGFP-transduced EDCs increased the amount of human IGF-1 transcript detected in the infarct and infarct border zone. Superior and sustained expression of IGF-1 was detected within the infarcted myocardium of animals treated with lvIGF-1-transduced EDCs until the end of follow-up (>21 days after intramyocardial injection). Off-target screening for human IGF-1 within serum collected 1, 7, and 14 days after EDC transplantation demonstrated that IGF-1 protein remained confined to the area of injection (Figure 4A), obviating concerns regarding widespread systemic effects.

Mice treated with lvIGF-1- or lvGFP-transduced EDCs 1 week after left anterior descending artery ligation demon-

strated greater myocardial function than PBS-treated controls, with superior benefits seen in lvIGF-1 EDC-treated mice (left ventricular ejection fraction: $41 \pm 2\%$ versus $37 \pm 1\%$; $P \leq 0.01$ versus lvGFP EDC-treated mice) (Figure 7B and Table S2). Histology performed 21 days after EDC transplantation confirmed these results with lvIGF-1 EDC-treated mice, demonstrating a 2.2 ± 0.4 -fold reduction in scar burden compared with lvGFP EDC-treated mice ($6 \pm 1\%$ versus $11 \pm 1\%$ scar, respectively; $P = 0.005$).

Although the transplant of lvIGF-1-transduced EDCs did not markedly influence the acute retention of transplanted cells, animals that received lvIGF-1-transduced EDCs demonstrated a progressive increase in long-term EDC retention such that EDC retention was increased 9.1 ± 3.6 -fold at 21 days after intramyocardial injection ($P = 0.05$ compared with injection of lvGFP-transduced EDCs) (Figures 6D and 4B). Random field analysis of myocardial sections from mice 21 days after EDC transplantation confirmed that lvIGF-1 EDC therapy boosted EDC engraftment compared with lvGFP EDC transplantation (8.5 ± 2.2 versus 3.2 ± 0.7 cells per random field, $P = 0.01$) (Figure 6D) without altering EDC ability to differentiate into cardiomyocyte, smooth muscle, or endothelial cell fate (Figure 6E and Figure S4C).

These data demonstrate that the transplant of lvIGF-1-transduced EDCs enhances myocardial repair, increasing the local content of IGF-1, and reduces ongoing loss of transplanted EDCs without altering transdifferentiation.

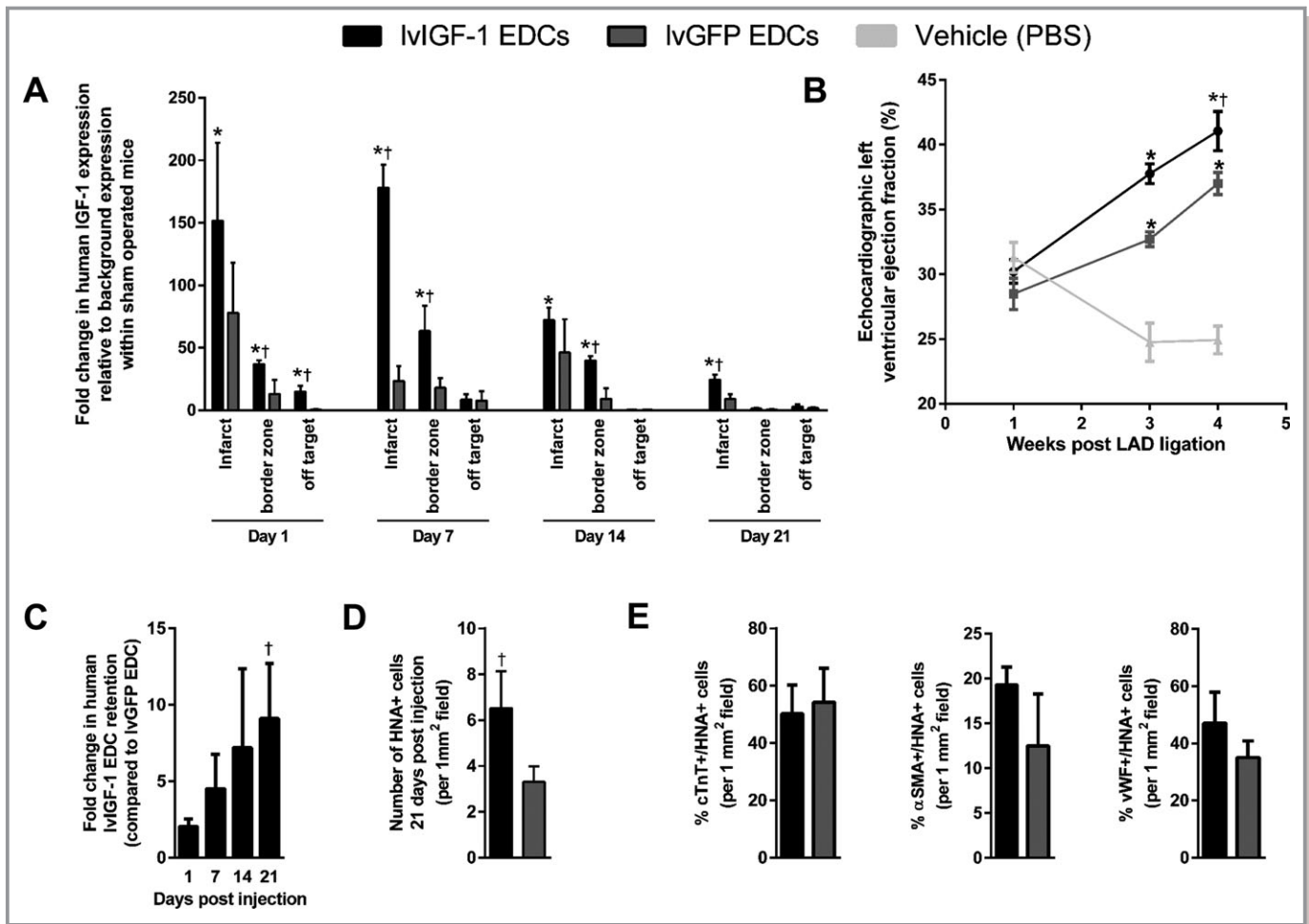


Figure 6. Transplantation of human EDCs genetically engineered to overexpress IGF-1 enhances postinfarct cardiac repair. A, Spatiotemporal expression of human IGF-1 transcript within infarct, border zone, and off-target ventricular tissue in mice following IvIGF-1 or IvGFP EDC transplantation compared with ventricular tissue from sham-operated mice. * $P \leq 0.05$ vs sham operated mice. † $P \leq 0.05$ vs IvGFP-transduced EDCs sampled at the same time point and region; $n=4$ mice with 3 technical repeats. B, Effect of IvGFP-transduced EDCs, IvIGF-1-transduced EDCs, and vehicle intramyocardial injection on NOD SCID mouse echocardiographic left ventricular ejection fraction. Significance was identified using a repeated-measured mixed model followed by post hoc testing using t tests with Bonferroni's correction. * $P \leq 0.05$ vs sham-operated mice. † $P \leq 0.05$ vs IvGFP-transduced EDCs sampled at the same time point; $n=8$ to 9 mice per treatment. C, Quantitative polymerase chain reaction of injected ventricles for retained human Alu sequences to document retention of human IvIGF-1 and IvGFP EDCs after cell transplantation. † $P \leq 0.05$ vs IvGFP-transduced EDCs; $n=3$ animals per sampling interval and group with 3 technical repeats per sample. D, Random field analysis of sections equidistant from the ligature for retained HNA+ cells at 21 days after injection. † $P \leq 0.05$ vs IvGFP-transduced EDCs; $n=3$ animals per sampling interval and group with 3 random fields per animal. E, Random field analysis of histological sections from the peri-infarct region quantifying the effect of IGF-1 overexpression on the ability of transplanted EDCs to differentiate into a cardiomyocyte (cTnT), smooth muscle (α SMA) or endothelial (vWF) lineage 21 days after IvIGF-1 or IvGFP EDC intramyocardial injection. $n=4$ mice with 3 random fields sampled. α SMA indicates α -smooth muscle actin; cTnT, cardiac troponin T; EDC, explant-derived cell; HNA, human nuclear antigen; IGF-1, insulin-like growth factor 1; IvGFP, lentiviral-mediated overexpression of the green fluorescent protein reporter; IvIGF-1, lentiviral-mediated overexpression of mature IGF-1 with green fluorescent protein; LAD, left anterior descending artery; vWF, von Willebrand Factor.

Overexpression of IGF-1 Reduced Apoptosis and Promoted Myocardial Regeneration

To evaluate the ability of IvIGF-1 EDCs to promote myocardial salvage, the expression of apoptotic transcripts within microdissected infarct and border zone regions was investigated 2 and 7 days after EDC injection (Figure 7A). Compared with transplants of IvGFP-transduced EDCs, the injection of

IvIGF-1-transduced EDCs reduced the expression of Bax and p53 by 3.4 ± 0.5 and 2.6 ± 0.9 -fold ($P \leq 0.05$) and promoted the expression of the antiapoptotic transcript Bcl-2 (2.2 ± 0.7 -fold; $P=0.1$). In vivo SPECT imaging performed before and 2 days after cell injection confirmed that the transplant of IvIGF-1-transduced EDCs reduced apoptosis within the ^{201}Tl -defined infarct region by $17 \pm 8\%$ ($P=0.0005$ versus baseline imaging), whereas treatment with IvGFP-transduced EDCs had no effect

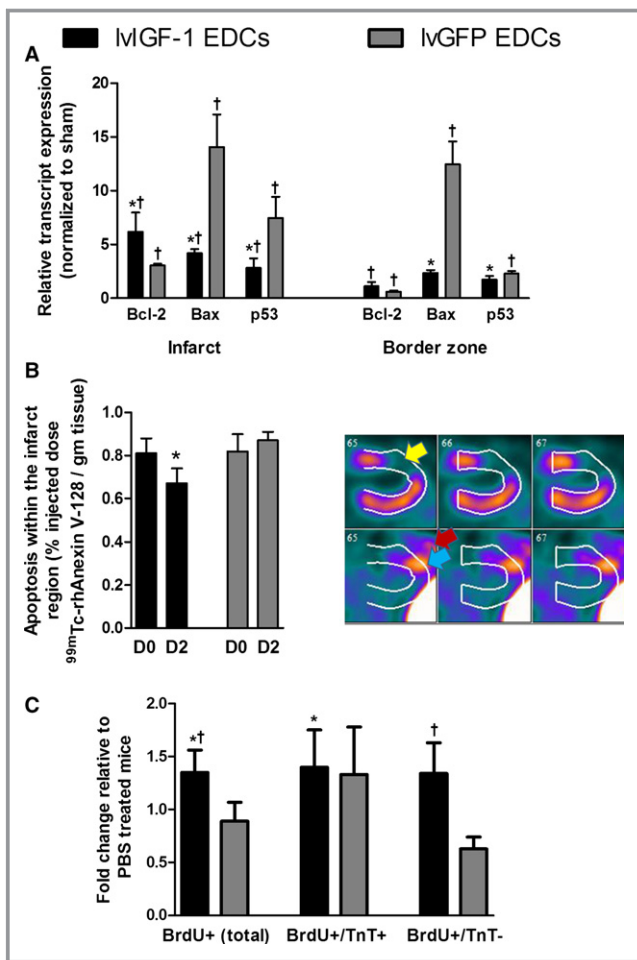


Figure 7. Transplantation of human EDCs genetically engineered to overexpress IGF-1 reduces apoptosis and promotes endogenous regeneration. A, Quantitative polymerase chain reaction of microdissected infarct and peri-infarct areas from mice treated with lvIGF-1- or lvGFP-transduced EDCs demonstrating reduced expression of apoptotic markers 7 days after EDC injection. * $P \leq 0.05$ vs lvGFP-transduced EDCs, † $P \leq 0.05$ vs sham-treated animals; $n=4$ mice with 3 technical repeats. B, Single-photon emission computed tomography quantification of apoptosis within the ^{201}Tl -defined infarct region before (D0) and 2 days after injection of lvIGF-1- or lvGFP-transduced EDCs (D2). Also shown are representative horizontal long-axis images from a mouse 2 days after injection of lvIGF-1 demonstrating ^{201}Tl perfusion images (upper panel) with myocardial infarction (yellow arrow) and $^{99\text{m}}\text{Tc}$ -rhAnnexin V-128 images (lower panel) with uptake in the area of infarction (blue arrow) and surgical site (red arrow). * $P \leq 0.05$ D2 vs D0; $n=3$ mice. C, NOD SCID mice injected with BrdU daily for 7 days after PBS or EDC injection demonstrate that transplant of lvIGF-1-transduced EDCs increase myocardial regeneration. * $P < 0.05$ vs PBS, † $P < 0.05$ vs lvGFP-transduced EDCs using random peri-infarct fields from 5 mice per treatment with 3 sections sampled per mouse ($n=15$ mice total). BrdU indicates bromodeoxyuridine; D, day; EDCs, explant-derived cells; IGF-1, insulin-like growth factor 1; lvGFP, lentiviral-mediated overexpression of the green fluorescent protein reporter; lvIGF-1, lentiviral-mediated overexpression of mature IGF-1 with green fluorescent protein; TnT, troponin T.

on imaged apoptosis (P value not significant versus baseline imaging and $P=0.083$ versus lvIGF-1-treated hearts) (Figure 7B). In a manner consistent with nuclear imaging and previous publications, transcript analysis of microdissected sections immediately after SPECT imaging confirmed that transplant of lvIGF-1 EDCs reduced expression of Bax and p53 (Figure S5).^{31–34} The influence of IGF-1 overexpression on endogenous repair was evaluated in a series of NOD SCID mice that received BrdU for 1 week after EDC or vehicle injection. As shown in Figure 7C, transplant of lvIGF-1 EDCs promoted proliferation of myocytes (BrdU+/troponin T-positive) and nonmyocytes (BrdU+/troponin T-negative) during the first week after cell injection. Taken together, these data suggest that transplant of lvIGF-1-transduced EDCs reduces apoptosis and the salvage of reversibly damaged tissue while promoting the generation of new myocardium.

Discussion

Although delivery of first-generation CSC therapy soon after myocardial injury improves cardiac function and reduces scarring,^{1,35} these benefits occur in the absence of robust cell engraftment,² hinting that CSC repair is mediated largely by the release of paracrine growth factors and their trophic actions on damaged tissue.^{3–5} Given that apoptosis plays a key role in myocardial cell loss after infarction,³⁶ it follows that maximizing the production of the prosurvival cytokine IGF-1 may improve the ability of transplanted cells to promote endogenous repair and elude anoikis. We demonstrated that the genetic engineering of EDCs to overexpress IGF-1 enabled transplanted cells to survive after injection, generate new myocardium, and promote the salvage of reversibly damaged tissue.

In a manner akin to other survival signaling pathways, we found that the IGF-1 axis was upregulated after ischemia. Interestingly, these transcripts were increased not only after the period of acute cell loss with infiltration of inflammatory cells (≈ 1 week in mice) but also during the fibrotic proliferation of scar maturation that ensues over the next 2 to 4 weeks in mice. Analogy to the postinfarct time course in humans would suggest that this period corresponds to 3 months after MI (ie, scar stabilization).³⁷ Although clinical evidence supporting myocardial responsiveness to IGF-1 is limited, the variable amount of IGF-1 produced by first-generation CSC products may provide a portion of benefits seen after transplantation, despite the treatment gap from MI to therapy dictated by the realities of autologous cell culture (weeks to months).¹ In this study, the peri-infarct area in mice was maximally responsive to IGF-1 at 7 days after left anterior descending artery ligation, justifying the timing of a cytokine-based therapy (≈ 1 month after MI in humans).^{37,38}

Like the myocardium, ex vivo proliferated c-Kit⁺ cells have been shown to be responsive to IGF-1 signaling, suggesting a role in autocrine/paracrine prosurvival effects.³⁹ In this study, we found that within the heterogeneous EDCs, IGF-1R and IR colocalized with all subpopulations, with a strong tendency to favor the cardiac (c-Kit⁺) and mesenchymal (CD90⁺) progenitor fractions. These results support the notion that IGF-1 primes EDCs to survive the harsh conditions in which CSCs would be expected to be operative by reducing ongoing anoikis, possibly through Akt and ERK/MAPK signaling.

Although deciphering the exact mechanism by which lvIGF-1–transduced EDCs promote myocardial repair is challenging, this study suggested that lvIGF-1–transduced EDCs persist longer after intramyocardial injection. As such, more cells are capable of (1) providing growth factors to stimulate endogenous repair and reduce neighboring cell loss and (2) transdifferentiating directly into new working myocardium. Clearly, more work is needed to understand the importance of EDC persistence in cell-mediated cardiac repair, but the identification of a novel paracrine means of boosting engraftment provides a promising way to increase transdifferentiation without recourse to overexpression of potentially oncogenic transcription factors.

This study had several important limitations including the use of lentiviral-mediated overexpression of IGF-1. Although this approach represents a relatively easy means of demonstrating proof of principle, clinical translation will require development and validation of good manufacturer practice-compatible cell culture and transgene expression. It is also unclear if antigenic selection and transduction of the CD90⁺ population alone is necessary to enhance cardiac repair. As outlined, this approach was chosen based on previous evidence that the CD90⁺ population contributes little to CDC-based cardiac repair^{14,16} and that transducing all cardiosphere-derived cells with hypoxia-inducible factor 1 α disrupts off-target cytokine production to ultimately impair cardiac repair.⁶ The timing of cell injection also represents a limitation of this work because the benefits conferred by an enhanced IGF-1 signal may not be realized when cells are administered to an extensively scarred myocardium (ie, >3 months after infarct) rather than to newly damaged or stunned tissue. Some of the statistical tests failed to reach significance; although we believe this is reflective of the underlying physiology, this finding could represent groups that were simply underpowered to detect small changes with high variability. Finally, more work will be needed to demonstrate the additive benefits conferred through cell-mediated delivery of IGF-1 to injured myocardium compared with sustained diffusion from impregnated biomaterials.

Genetic enhancement of IGF-1 in human CSCs improves cardiac repair when delivered 7 days after MI in mice. The genetic priming of CSCs with IGF-1 promotes transplant cell

survival, boosts long-term CSC engraftment, and delivers sustained local IGF-1 to damaged myocardium. This increase was associated with the upregulation of prosurvival factors and the reduction of apoptosis to improve myocardial function and the salvage of damaged myocardium. This paper is the first example in the literature to show that paracrine engineering of human CSCs can improve cardiac repair, salvage reversibly damaged myocardium, promote the generation new myocardial cells, and increase long-term engraftment of transplanted CSCs by reducing ongoing cell loss. Most important, this study is firmly grounded in the real world by culturing stem cells directly from patients who will likely need this therapy in the future.

Acknowledgments

We would like to acknowledge Richard Seymour for performing mouse surgeries.

Sources of Funding

This work was supported by the Canadian Institutes of Health Research (Operating Grant 229694) and the Heart and Stroke Foundation of Canada (G-14-0006113). Dr Davis is funded by the Canadian Institutes of Health Research (Clinician Scientist Award MC2-121291).

Disclosures

None.

References

- Makkar RR, Smith RR, Cheng K, Malliaras K, Thomson LE, Berman D, Czer LS, Marban L, Mendizabal A, Johnston PV, Russell SD, Schuleri KH, Lardo AC, Gerstenblith G, Marban E. Intracoronary cardiosphere-derived cells for heart regeneration after myocardial infarction (CADUCEUS): a prospective, randomised phase 1 trial. *Lancet*. 2012;379:895–904.
- Terrovitis J, Kwok KF, Lautamaki R, Engles JM, Barth AS, Kizana E, Miake J, Leppo MK, Fox J, Seidel J, Pomper M, Wahl RL, Tsui B, Bengel F, Marban E, Abraham MR. Ectopic expression of the sodium-iodide symporter enables imaging of transplanted cardiac stem cells in vivo by single-photon emission computed tomography or positron emission tomography. *J Am Coll Cardiol*. 2008;52:1652–1660.
- Chimenti I, Smith RR, Li TS, Gerstenblith G, Messina E, Giacomello A, Marban E. Relative roles of direct regeneration versus paracrine effects of human cardiosphere-derived cells transplanted into infarcted mice. *Circ Res*. 2010;106:971–980.
- Malliaras K, Zhang Y, Seinfeld J, Galang G, Tseliou E, Cheng K, Sun B, Aminzadeh M, Marban E. Cardiomyocyte proliferation and progenitor cell recruitment underlie therapeutic regeneration after myocardial infarction in the adult mouse heart. *EMBO Mol Med*. 2013;5:191–209.
- Malliaras K, Ibrahim A, Tseliou E, Liu W, Sun B, Middleton RC, Seinfeld J, Wang L, Sharifi BG, Marban E. Stimulation of endogenous cardioblasts by exogenous cell therapy after myocardial infarction. *EMBO Mol Med*. 2014;6:760–777.
- Bonios M, Chang CY, Terrovitis J, Pinheiro A, Barth A, Dong P, Santalucia M, Foster DB, Raman V, Abraham TP, Abraham MR. Constitutive HIF-1 α expression blunts the beneficial effects of cardiosphere-derived cell therapy in the heart by altering paracrine factor balance. *J Cardiovasc Transl Res*. 2011;4:363–372.

7. Laron Z. Insulin-like growth factor 1 (IGF-1): a growth hormone. *Mol Pathol.* 2001;54:311–316.
8. Liu JL, LeRoith D. Insulin-like growth factor I is essential for postnatal growth in response to growth hormone. *Endocrinology.* 1999;140:5178–5184.
9. Ellison GM, Torella D, Dellegrottaglie S, Perez-Martinez C, de Perez PA, Vicinanza C, Purushothaman S, Galuppo V, Iaconetti C, Waring CD, Smith A, Torella M, Cuellas RC, Gonzalo-Orden JM, Agosti V, Indolfi C, Galinanes M, Fernandez-Vazquez F, Nadal-Ginard B. Endogenous cardiac stem cell activation by insulin-like growth factor-1/hepatocyte growth factor intracoronary injection fosters survival and regeneration of the infarcted pig heart. *J Am Coll Cardiol.* 2011;58:977–986.
10. Koudstaal S, Bastings MM, Feyen DA, Waring CD, van Slochteren FJ, Dankers PY, Torella D, Sluijter JP, Nadal-Ginard B, Doevendans PA, Ellison GM, Chamuleau SA. Sustained delivery of insulin-like growth factor-1/hepatocyte growth factor stimulates endogenous cardiac repair in the chronic infarcted pig heart. *J Cardiovasc Transl Res.* 2014;7:232–241.
11. Haider HK, Jiang S, Idris NM, Ashraf M. IGF-1-overexpressing mesenchymal stem cells accelerate bone marrow stem cell mobilization via paracrine activation of SDF-1alpha/CXCR4 signaling to promote myocardial repair. *Circ Res.* 2008;103:1300–1308.
12. Smith RR, Barile L, Cho HC, Leppo MK, Hare JM, Messina E, Giacomello A, Abraham MR, Marban E. Regenerative potential of cardiosphere-derived cells expanded from percutaneous endomyocardial biopsy specimens. *Circulation.* 2007;115:896–908.
13. Bearzi C, Rota M, Hosoda T, Tillmanns J, Nascimbene A, De Angelis A, Yasuzawa-Amano S, Trofimova I, Siggins RW, Lecapitaine N, Cascapera S, Beltrami AP, D'Alessandro DA, Zias E, Quaini F, Urbanek K, Michler RE, Bolli R, Kajstura J, Leri A, Anversa P. Human cardiac stem cells. *Proc Natl Acad Sci USA.* 2007;104:14068–14073.
14. Gago-Lopez N, Awaji O, Zhang Y, Ko C, Nsair A, Liem D, Stempien-Otero A, MacLellan WR. THY-1 receptor expression differentiates cardiosphere-derived cells with divergent cardiogenic differentiation potential. *Stem Cell Reports.* 2014;2:576–591.
15. Sen S, Merchan J, Dean J, Li M, Gavin M, Silver M, Tkebuchava T, Yoon YS, Rasko JE, Aikawa R. Autologous transplantation of endothelial progenitor cells genetically modified by adeno-associated viral vector delivering insulin-like growth factor-1 gene after myocardial infarction. *Hum Gene Ther.* 2010;21:1327–1334.
16. Cheng K, Ibrahim A, Hensley MT, Shen D, Sun B, Middleton R, Liu W, Smith RR, Marban E. Relative roles of CD90 and c-kit to the regenerative efficacy of cardiosphere-derived cells in humans and in a mouse model of myocardial infarction. *J Am Heart Assoc.* 2014;3:e001260 doi: 10.1161/JAHA.114.001260.
17. Davis DR, Kizana E, Terrovitis J, Barth AS, Zhang Y, Smith RR, Miake J, Marban E. Isolation and expansion of functionally-competent cardiac progenitor cells directly from heart biopsies. *J Mol Cell Cardiol.* 2010;49:312–321.
18. Latham N, Ye B, Jackson R, Lam B, Kuraitis D, Ruel M, Suuronen EJ, Stewart DJ, Davis DR. Human blood and cardiac stem cells synergize to enhance cardiac repair when cotransplanted into ischemic myocardium. *Circulation.* 2013;128:S1–S8.
19. Mayfield AE, Tilokee EL, Latham N, McNeill B, Lam BK, Ruel M, Suuronen EJ, Courtman DW, Stewart DJ, Davis DR. The effect of encapsulation of cardiac stem cells within matrix-enriched hydrogel capsules on cell survival, post-ischemic cell retention and cardiac function. *Biomaterials.* 2014;35:133–142.
20. Davis DR, Smith RR, Marban E. Human cardiospheres are a source of stem cells with cardiomyogenic potential. *Stem Cells.* 2010;28:903–904.
21. Davis DR, Zhang Y, Smith RR, Cheng K, Terrovitis J, Malliaras K, Li TS, White A, Makkar R, Marban E. Validation of the cardiosphere method to culture cardiac progenitor cells from myocardial tissue. *PLoS One.* 2009;4:e7195.
22. Tiscornia G, Singer O, Verma IM. Production and purification of lentiviral vectors. *Nat Protoc.* 2006;1:241–245.
23. Sastry L, Johnson T, Hobson MJ, Smucker B, Cornetta K. Titering lentiviral vectors: comparison of DNA, RNA and marker expression methods. *Gene Ther.* 2002;9:1155–1162.
24. Molgat AS, Tilokee EL, Rafatian G, Vulesevic B, Ruel M, Milne R, Suuronen EJ, Davis DR. Hyperglycemia inhibits cardiac stem cell-mediated cardiac repair and angiogenic capacity. *Circulation.* 2014;130:S70–S76.
25. Munoz JR, Stoutenger BR, Robinson AP, Spees JL, Prockop DJ. Human stem/progenitor cells from bone marrow promote neurogenesis of endogenous neural stem cells in the hippocampus of mice. *Proc Natl Acad Sci USA.* 2005;102:18171–18176.
26. Li T-S, Lee S-T, Matsushita S, Davis DR, Zhang Y, Smith RR, Marban E. Cardiospheres recapitulate a niche-like microenvironment rich in stemness and cell-matrix interactions, rationalizing their enhanced functional potency for myocardial repair. *Stem Cells.* 2010;105:2088–2098.
27. Brown RD, Ambler SK, Mitchell MD, Long CS. The cardiac fibroblast: therapeutic target in myocardial remodeling and failure. *Annu Rev Pharmacol Toxicol.* 2005;45:657–687.
28. Bryant JE, Shamhart PE, Luther DJ, Olson ER, Koshy JC, Costic DJ, Mohile MV, Dockry M, Doane KJ, Meszaros JG. Cardiac myofibroblast differentiation is attenuated by alpha(3) integrin blockade: potential role in post-MI remodeling. *J Mol Cell Cardiol.* 2009;46:186–192.
29. Fedak PW, Bai L, Turnbull J, Ngu J, Narine K, Duff HJ. Cell therapy limits myofibroblast differentiation and structural cardiac remodeling: basic fibroblast growth factor-mediated paracrine mechanism. *Circ Heart Fail.* 2012;5:349–356.
30. Shavlakadze T, White J, Hoh JF, Rosenthal N, Grounds MD. Targeted expression of insulin-like growth factor-I reduces early myofiber necrosis in dystrophic mdx mice. *Mol Ther.* 2004;10:829–843.
31. Taki J, Higuchi T, Kawashima A, Tait JF, Kinuya S, Muramori A, Matsunari I, Nakajima K, Tonami N, Strauss HW. Detection of cardiomyocyte death in a rat model of ischemia and reperfusion using ^{99m}Tc-labeled annexin V. *J Nucl Med.* 2004;45:1536–1541.
32. Taki J, Higuchi T, Kawashima A, Fukuoka M, Kayano D, Tait JF, Matsunari I, Nakajima K, Kinuya S, Strauss HW. Effect of postconditioning on myocardial ^{99m}Tc-annexin-V uptake: comparison with ischemic preconditioning and caspase inhibitor treatment. *J Nucl Med.* 2007;48:1301–1307.
33. Taki J, Higuchi T, Kawashima A, Tait JF, Muramori A, Matsunari I, Nakajima K, Vanderheyden JL, Strauss HW. (^{99m}Tc)annexin-V uptake in a rat model of variable ischemic severity and reperfusion time. *Circ J.* 2007;71:1141–1146.
34. Zhao Y, Zhao S, Kuge Y, Strauss HW, Blankenberg FG, Tamaki N. Attenuation of apoptosis by telmisartan in atherosclerotic plaques of apolipoprotein E-/- mice: evaluation using technetium ^{99m}-annexin A5. *Mol Imaging.* 2013;12:300–309.
35. Bolli R, Chugh AR, D'Amario D, Loughran JH, Stoddard MF, Ikram S, Beache GM, Wagner SG, Leri A, Hosoda T, Sanada F, Elmore JB, Goichberg P, Cappetta D, Solankhi NK, Fahsah I, Rokosh DG, Slaughter MS, Kajstura J, Anversa P. Cardiac stem cells in patients with ischaemic cardiomyopathy (SCIPIO): initial results of a randomised phase 1 trial. *Lancet.* 2011;378:1847–1857.
36. Anversa P, Cheng W, Liu Y, Leri A, Redaelli G, Kajstura J. Apoptosis and myocardial infarction. *Basic Res Cardiol.* 1998;93(suppl 3):8–12.
37. Fujiwara H, Matsuda M, Fujiwara Y, Ishida M, Kawamura A, Takemura G, Kida M, Uegaito T, Tanaka M, Horike K. Infarct size and the protection of ischemic myocardium in pig, dog and human. *Jpn Circ J.* 1989;53:1092–1097.
38. Nian M, Lee P, Khaper N, Liu P. Inflammatory cytokines and postmyocardial infarction remodeling. *Circ Res.* 2004;94:1543–1553.
39. D'Amario D, Fiorini C, Campbell PM, Goichberg P, Sanada F, Zheng H, Hosoda T, Rota M, Connell JM, Gallegos RP, Welt FG, Givertz MM, Mitchell RN, Leri A, Kajstura J, Pfeffer MA, Anversa P. Functionally competent cardiac stem cells can be isolated from endomyocardial biopsies of patients with advanced cardiomyopathies. *Circ Res.* 2011;108:857–861.